

Silicon-on-Insulator Polarization Rotator Based on a Symmetry Breaking Silicon Overlay

Diedrik Vermeulen, *Student Member, IEEE*, Shankar Selvaraja, *Member, IEEE*, Peter Verheyen, Philippe Absil, Wim Bogaerts, *Member, IEEE*, Dries Van Thourhout, *Member, IEEE*, and Gunther Roelkens, *Member, IEEE*

Abstract—We demonstrate a polarization rotator fabricated using a 4 etch-step complementary metal–oxide–semiconductor (CMOS)-compatible process including layer depositions on a silicon-on-insulator wafer. The measured polarization rotation efficiency is -0.51 dB over a wavelength range of 80 nm. A robustness investigation shows that the design is compatible with CMOS fabrication capabilities.

Index Terms—Polarization rotator, silicon-on-insulator (SOI).

I. INTRODUCTION

SILICON-ON-INSULATOR (SOI) photonic integrated circuits (PICs) are rapidly becoming a key technology for low-cost and high-volume oriented photonic applications. By organizing Multi Project Wafer (MPW) shuttles silicon PIC prototyping can be realized at an affordable cost while at the same time guaranteeing specifications comparable to Complementary Metal Oxide Semiconductor (CMOS) circuits. This fabless model also allows the research community to focus on device and application ideas, design and characterization. In the first stage of the Silicon Photonics era much research was focused on proof-of-concept circuits, solving the most stringent problems like fiber coupling and mimicking photonic devices developed on other platforms such as *InP* and polymer waveguide circuits. Nowadays, researchers are focusing on methods to optimize existing photonic components and on expanding the set of photonic functionalities. Polarization independent functionalities are in most cases not an option due to the highly birefringent waveguides in high index contrast SOI waveguides. Polarization diversity on the other hand requires a broadband and efficient polarization rotator which remained until recently a missing link.

An early polarization diversity circuit [1] made use of 2-dimensional grating fiber couplers which act as a fiber

coupler, polarization splitter and polarization rotator at the same time. Unfortunately, their efficiency is rather low, around -7 dB, and their 1-dB bandwidth is only 20 nm. Another polarization diversity circuit [2] uses an off-axis double core structure of a small silicon wire and large *SiN* wire ($0.84 \mu\text{m} \times 0.84 \mu\text{m}$) as polarization rotator. Achieving such a thick high quality *SiN* in a CMOS environment using Low Pressure Chemical Vapor Deposition (LPCVD) is not obvious. Furthermore, if the PIC contains electro-optic components or photodetectors, the implementation of such a structure is non-trivial. A mode-evolution-based polarization rotator was successfully demonstrated in [3], but with insertion losses up to 5 dB. Large core waveguides ($\sim 2 \mu\text{m}$) with angled sidewalls were investigated in [4]. An interesting development are polarization rotators based on asymmetrical directional couplers ([5], [6]). These structures are very simple and require only a single etch step. However, the waveguide structure needs to be vertically asymmetrical to achieve coupling between both polarizations. In [7] a compact polarization rotator was proposed using a straight asymmetric shallow etch in a square strip waveguide configuration. In what follows we will elaborate on this report by experimentally demonstrating a slightly modified polarization rotator configuration and investigate the robustness of this structure. Furthermore, the fabrication process is exactly the same as for the highly efficient grating couplers reported in [8], thereby permitting cointegration of both polarization rotators and high-efficiency grating couplers.

II. DESIGN AND FABRICATION PROCESS

The complete fabrication process is done in a CMOS pilot line with 193 nm deep ultraviolet (DUV) lithography. First a 5 nm silicon oxide layer is thermally grown on a 200 nm SOI wafer with a buried oxide layer thickness of $2 \mu\text{m}$ and a crystalline silicon layer thickness of 220 nm. In a second step an amorphous silicon layer of 160 nm is deposited and a deep etch is performed through the amorphous silicon and oxide layer reaching 70 nm into the crystalline silicon layer. This is used to define the slits of the high efficiency grating couplers. Next, the amorphous silicon is removed where necessary and the thermally grown oxide layer in the first step will now act as an etch stop layer in order to not affect the underlying crystalline silicon. A shallow etch of 70 nm in the 220 nm crystalline silicon layer is introduced to achieve low loss and robust spectral filter components. Finally, the waveguide trenches are defined by a 220 nm etch and the amorphous silicon is annealed after which it becomes polycrystalline silicon.

Manuscript received October 7, 2011; revised November 9, 2011; accepted December 20, 2011. Date of current version February 29, 2012. This work was supported in part by the Dutch Smartmix-Memphis Project and in part by the European Union in the FP7-ICT-HELIOS Project. The work of D. Vermeulen was supported in part by a grant from the Institute for the Promotion of Innovation by Science and Technology, Flanders (IWT).

D. Vermeulen, S. Selvaraja, W. Bogaerts, D. Van Thourhout, and G. Roelkens are with the Department of Information Technology, Photonics Research Group, Ghent University-IMEC, Gent B-9000, Belgium (e-mail: diedrik.vermeulen@intec.ugent.be; shankar@intec.ugent.be; wim.bogaerts@intec.ugent.be; dries.vanthourhout@intec.ugent.be; gunther.roelkens@intec.ugent.be).

P. Verheyen and P. Absil are with IMEC, Leuven 3001, Belgium (e-mail: verheyen@imec.be; absilp@imec.be).

Color versions of one or more of the figures in this letter are available online at <http://ieeexplore.ieee.org>.

Digital Object Identifier 10.1109/LPT.2011.2181944

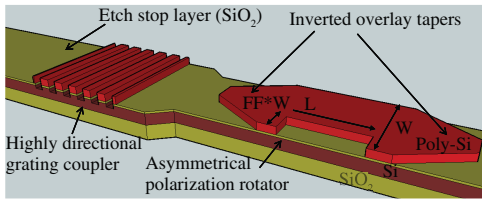


Fig. 1. Artist's impression of a highly directional fiber coupler and asymmetrical polarization rotator fabricated within the same process flow. (Dimensions are not to scale)

In Fig. 1 an artist's impression is shown of a high-efficiency grating coupler and a polarization rotator, both compatible with the aforementioned process flow. The polarization rotator design is based on symmetry breaking of a waveguide with an almost square waveguide profile. An inverted taper, defined in the silicon overlay, is used as an adiabatic transition between a 450 nm wide *Si* waveguide with a height of 220 nm and an equally wide waveguide with a silicon overlay. This double patterned strip waveguide has a combined thickness of 380 nm and is formed by 220 nm crystalline silicon and a 160 nm polycrystalline silicon with 5 nm thermally grown silicon oxide in between. According to simulations the 100 nm wide tip of the inverted taper would introduce no loss and a 0.4 dB loss for TE- (Transverse Electric) and TM-polarized (Transverse Magnetic) light respectively. The actual polarization rotator is formed by a 405 nm wide waveguide with an asymmetrical overlay. For a fill factor of 75% for the silicon overlay, a TE or TM polarized fundamental mode couples equally to both 50% TE/TM polarized hybrid modes of the asymmetrical waveguide at the symmetric-asymmetric waveguide interface. After propagation over 7.6 μm , both asymmetrical hybridly polarized waveguide modes will couple to the fundamental TM mode in the output waveguide when a TE mode is launched (and vice versa when a TM mode is launched) at the asymmetric-symmetric waveguide interface, thereby obtaining polarization conversion, see Fig. 2. The short conversion length is a consequence of the large difference in propagation constants of the two beating modes ($\beta_{H1} - \beta_{H2} = 10.12 \mu\text{m}^{-1} - 9.70 \mu\text{m}^{-1} = 0.42 \mu\text{m}^{-1}$) in the asymmetric waveguide and results in a large (> 100 nm from simulation) polarization conversion optical bandwidth. SEM pictures of the fabricated polarization rotator are shown in Fig. 3(a) and 3(b).

III. MEASUREMENTS

The polarization rotators were characterized by means of grating couplers. These are highly polarization dependent structures and act as polarization filtering couplers with an extinction ratio of around 50 dB. The periods of the grating couplers were 630 nm and 1040 nm for coupling respectively TE- and TM-polarized light. First the inverted overlay tapers with a designed tip width of 100 nm were characterized by measuring the TE and TM insertion loss of a waveguide which is tapered to a strip waveguide with silicon overlay and back. The measured insertion loss for the inverted taper is smaller than 0.1 dB for both TE- and TM- polarized light which is explained by the reduced tip width of 50 nm of the fabricated

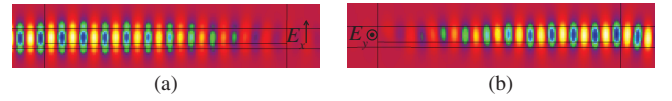


Fig. 2. Top view field plots of the polarization rotator, obtained using a fully vectorial eigenmode expansion tool. (a) E_x field (TE polarization). (b) E_y field (TM polarization).

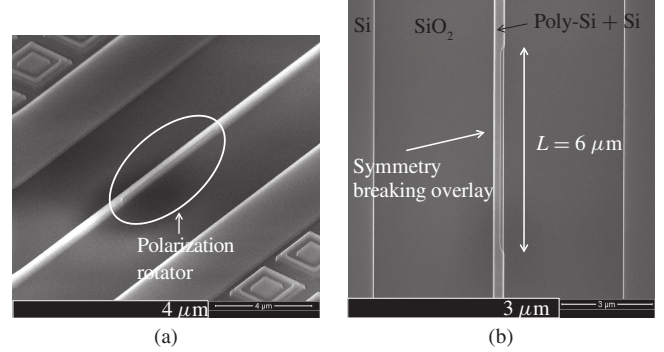


Fig. 3. SEM images of the fabricated polarization rotator. (a) Bird's eye view of a realized polarization rotator. (b) Top view: a poly-Si overlay breaks the symmetry of the waveguide such that after a propagation over L of 6 μm , almost total polarization conversion is achieved.

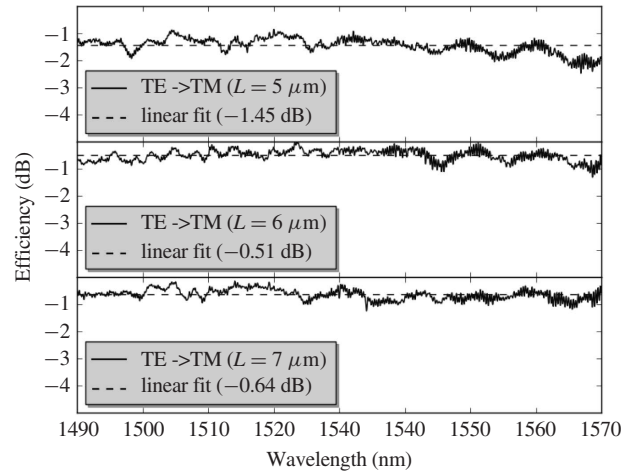


Fig. 4. Measurements of the polarization rotator ($W = 405$ nm, $FF = 75\%$) TE to TM insertion loss for different rotator lengths L .

device. The polarization rotators are characterized by measuring the TE to TM transmission $T_{TE \rightarrow TM}$, normalized with the reference measurements of the grating couplers. The TE to TM insertion loss is the sum of the intrinsic loss of the polarization rotator and the TE to TE transmission $T_{TE \rightarrow TE}$ (crosstalk). Simulations show that the insertion loss is very low, so we can assume that $T_{TE \rightarrow TE} = 1 - T_{TE \rightarrow TM}$ and that the polarization conversion efficiency (PCE), defined by $PCE = T_{TE \rightarrow TM} / (T_{TE \rightarrow TE} + T_{TE \rightarrow TM})$, equals $T_{TE \rightarrow TM}$. The measurement results of polarization rotators with a width W of 405 nm and fill factor FF of 75% are plotted in Fig. 4. The optimal structure has a length L between 6 μm and 7 μm , which is in relatively good agreement with our simulations where we found that the optimal length is 7.6 μm . The highest measured PCE is -0.51 dB for a rotator length of 6 μm .

Furthermore, the high PCE was measured over a broad wavelength range of 80 nm, equal to the 3-dB bandwidth of the

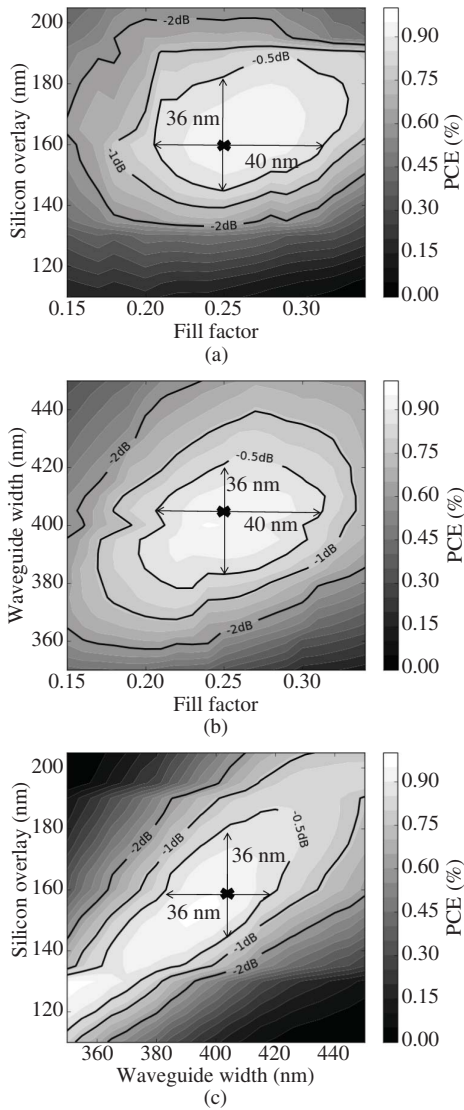


Fig. 5. Polarization rotator robustness investigation as a function of the critical parameters. The contour lines are the PCE penalties with respect to the highest PCE of the device. (a) PCE as a function of the silicon overlay thickness and fill factor. (b) PCE as a function of the waveguide width W and fill factor FF . (c) PCE as a function of the waveguide width W and silicon overlay thickness.

grating coupler. The upper limit for the crosstalk ($T_{TE \rightarrow TE} < 1 - T_{TE \rightarrow TM}$) is -9.55 dB. For practical applications, this residual crosstalk can be easily removed by implementing a polarization filter or polarization splitter such as a directional coupler, multi-mode interferometer (MMI) or sharp bend.

IV. ROBUSTNESS

The robustness was assessed by scanning the critical parameter space of the fabricated polarization rotator ($W = 405$ nm, $FF = 75\%$, $L = 7$ μ m) where the rotator length L is kept constant. The cross in the robustness figures indicates the parameters of the fabricated polarization rotator with a simulated PCE of 95% or -0.22 dB. In Fig. 5(a) the PCE is

plotted versus the fill factor FF and silicon overlay thickness. For a -0.5 dB PCE penalty, the duty cycle may vary $\pm 5\%$ which translates into to a mask alignment tolerance of ± 20 nm. The silicon overlay thickness -0.5 dB PCE tolerance is $+21$ nm and -15 nm. Note that the etch depth is fixed in our case at exactly the silicon overlay thickness due to the SiO_2 etch stop layer (see Fig. 1) which attributes to the overall robustness of our component. Nonetheless, it introduces an extra 0.2 dB PCE penalty for a 5 nm thick silicon oxide etch stop layer. The PCE is plotted as a function of the waveguide width and fill factor in Fig. 5(b) and as a function of the overlay thickness and waveguide width in Fig. 5(c). The -0.5 dB PCE tolerance is $+15$ nm and -21 nm for the waveguide width. These robustness specifications are compatible with CMOS fabrication capabilities.

V. CONCLUSION

We have experimentally realized a high efficiency and broadband integrated polarization rotator with a polarization conversion efficiency of -0.51 dB over a bandwidth of 80 nm. An advanced passive SOI 4 etch-step process flow was used for the fabrication. With this process, 4 different layer thicknesses can be resolved and high-efficiency grating couplers using a silicon overlay could be integrated on the same optical chip. Furthermore, the accompanied extra design freedom offers an excellent tool to optimize other optical integrated components such as splitters, filters and optical interconnects. Additionally, we investigated the robustness and have shown that the design has -0.5 dB PCE tolerances which are compatible with standard CMOS fabrication tolerances. The crosstalk is -9.55 dB and could be easily improved by using a polarization splitter or filter, e.g. a directional coupler, MMI or sharp bend.

REFERENCES

- [1] W. Bogaerts, D. Taillaert, P. Dumon, D. Van Thourhout, R. Baets, and E. Pluk, "A polarization-diversity wavelength duplexer circuit in silicon-on-insulator photonic wires," *Opt. Express*, vol. 15, no. 4, pp. 1567–1578, 2007.
- [2] H. Fukuda, K. Yamada, T. Tsuchizawa, T. Watanabe, H. Shinjima, and S.-I. Itabashi, "Silicon photonic circuit with polarization diversity," *Opt. Express*, vol. 16, no. 7, pp. 4872–4880, 2008.
- [3] J. Zhang, M. Yu, G.-Q. Lo, and D.-L. Kwong, "Silicon-waveguide-based mode evolution polarization rotator," *IEEE J. Sel. Topics Quantum Electron.*, vol. 16, no. 1, pp. 53–60, Jan./Feb. 2010.
- [4] H. Deng, D. O. Yevick, C. Brooks, and P. E. Jessop, "Fabrication tolerance of asymmetric silicon-on-insulator polarization rotators," *J. Opt. Soc. Amer. A, Opt., Image Sci., Vis.*, vol. 23, no. 7, pp. 1741–1745, 2006.
- [5] L. Liu, Y. Ding, K. Yvind, and J. R. M. Hvam, "Silicon-on-insulator polarization splitting and rotating device for polarization diversity circuits," *Opt. Express*, vol. 19, no. 13, pp. 12646–12651, 2011.
- [6] D. Dai and J. E. Bowers, "Novel concept for ultracompact polarization splitter-rotator based on silicon nanowires," *Opt. Express*, vol. 19, no. 11, pp. 10940–10949, 2011.
- [7] Z. Wang and D. Dai, "Ultrasmall Si-nanowire-based polarization rotator," *J. Opt. Soc. Amer. B*, vol. 25, no. 5, pp. 747–753, 2008.
- [8] D. Vermeulen, *et al.*, "High-efficiency fiber-to-chip grating couplers realized using an advanced CMOS-compatible silicon-on-insulator platform," *Opt. Express*, vol. 18, no. 17, pp. 18278–18283, 2010.